CrossMark

**ORIGINAL PAPER**

# Dry Sliding Wear Behaviour of Aluminium Al–Si12Cu/TiB$_2$ Metal Matrix Composite Using Response Surface Methodology

**N. Radhika[1] · R. Raghu[1]**

**Abstract**  An aluminium Al–Si12Cu/TiB$_2$ metal matrix composite was fabricated using the liquid metallurgy route, and its dry sliding wear characteristics were investigated under various sliding parameters. The titanium diboride (TiB$_2$) particles (10 wt%, average size 50–60 μm) were incorporated into the matrix and its microstructural characteristic was examined. A five-level central composite design experiment was developed using response surface methodology; parameters such as load, velocity and sliding distance were varied in the range of 10–50 N, 1–5 m/s and 500–2500 m, respectively. Dry sliding wear tests were performed as per the experimental design using a pin-on-disc tribometer at room temperature. Significance tests, analyses of variance and confirmatory tests were performed to validate the developed model. Study of the microstructural characteristics revealed uniform dispersion of the reinforcement particles throughout the composite. The regression result showed that the developed model performed well in relating the wear process parameters with the response and predicting the wear behaviour of the composite. The surface plot showed that wear rate increased with increasing load at all velocities and distances, and decreased with increasing sliding distance. In the case of velocity, the wear rate decreased initially, increasing after the transition velocity had been reached. Scanning electron microscopy analysis revealed severe wear at a high load due to a higher level of deformation of the composite surface.

✉ N. Radhika
   n_radhika1@cb.amrita.edu

[1]  Department of Mechanical Engineering, Amrita Vishwa
     Vidyapeetham, Ettimadai, Coimbatore, Tamil Nadu 641112,
     India

## 1 Introduction

Many composite materials with industrial applications have been developed over the years, including the more recently developed aluminium metal matrix composite (AMMC) materials that are being increasingly used for applications in the automotive, aerospace and defense industries. The incorporation of hard particulates in the aluminium alloys increase the suitability of these alloys in wear applications due to an improved strength, better stiffness and high wear resistance [1]. Various processes for fabricating AMMCs with different reinforcements have been proposed [2], where the liquid metallurgy technique ultimately proposed to be the simplest, most flexible and most economical technique for their fabrication [3].

Sucitharan et al. [4] investigated the characteristics of aluminium/zircon sand metal matrix composites (MMCs) obtained by stir casting and reported that process parameters, such as stirring speed, stirring time, particle-preheating temperature and volume percentage (vol%) of the reinforcement, should be controlled carefully for the successful incorporation of the reinforcement particles into the matrix. Stir casting is a commonly employed process for fabricating aluminium/fused silica composites. Analysis of the microstructural characteristics of composites produced by stir casting revealed that this process achieves the fine dispersion of the reinforcement particles which facilitates the production of materials with the required mechanical and tribological properties [5]. An aluminium/titanium diboride (TiB$_2$) composite produced by stir casting has been investigated for its mechanical properties and

its performance compared with that of the commercial aluminium alloy. The results revealed that the aluminium/ $TiB_2$ composite showed a 25 % improvement in hardness and a 10 % improvement in impact strength over the un-reinforced aluminium alloy [6].

Bhaskar and Sharief [7] investigated an aluminium/beryl composite for its dry sliding wear characteristics under the control of parameters such as applied load, sliding speed and sliding distance. These authors reported that both sliding distance and load had a major effect in controlling the dry sliding wear characteristics of the composite. The dry sliding wear of aluminium hybrid composites has been investigated using the design of experiments (DOE) technique to study the influence of factors on the wear rate; the results showed that in addition to individual parameters, the interaction term of the factors also predominantly affected the wear rate [8]. Response surface methodology (RSM) is an often applied approach to study the abrasive wear behaviour of a fibre-reinforced polymer composite under various loads, different volume percentages of reinforcement and varied sliding velocities. Using this approach, Mishra [9] found that the model developed using RSM is good in predicting the results with high accuracy. Using RSM, Bayhan and Ohel [10] studied the wear behaviour of Al–Si7Mg/silicon carbide (SiC) composites with different reinforcement content and at various sliding distances and determined the optimum reinforcement content (13 wt%) and sliding distance (595 m) which resulted in minimum wear rate.

To date, very few studies have been published on the wear behaviour of $TiB_2$-reinforced AMMC. Therefore, the aim of this study was to use RSM to elucidate the dry sliding wear behaviour of $TiB_2$ (10 wt%)-reinforced Al–Si12Cu MMC fabricated using the liquid metallurgy technique.

## 2 Materials and Methods

### 2.1 Selection of Materials

The Al–Si12Cu alloy was selected for study based on its vast tribological applications, in particular for its use in pistons. $TiB_2$, in the form of (10 wt%) particles with an average size of 50–60 μm, was selected as reinforcement due to its high degree of hardness and high wear resistance. The density of the alloy and the reinforcement was 2.70 and 4.52 gm/cm$^3$, respectively. The chemical composition of the alloy is given in Table 1.

### 2.2 Composite Fabrication

The aluminium ingots were sliced into pieces, loaded into the graphite crucible and places in an electrical resistance

**Table 1** Chemical composition of the Al–Si12Cu alloy

| Chemical composition | % |
| --- | --- |
| Al | 83.40 |
| Si | 10.90 |
| Fe | 0.52 |
| Cu | 1.31 |
| Mg | 1.05 |
| Ni | 2.32 |
| Others (Mn, Cr, Zn, Sn, Ti, Pb, Ca) | 0.50 |

furnace for melting. Following attainment of the molten stage, the preheated $TiB_2$ reinforcement particles were added manually through the hopper setup of the furnace. The furnace was specially equipped with a stirrer setup to disperse the reinforcement particles in the molten metal. To achieve the uniform dispersion of the reinforcement particles in the molten metal, the molten metal was stirred at 200 rpm and mixed for 5 min at 760 °C before being poured into the preheated metallic die. The cast component was ejected from the die following solidification at room temperature.

### 2.3 Microstructural Examination

Specimens of the cast component were taken for microstructural analysis in order to verify uniform dispersion of the reinforcement particles in the matrix. These specimens were first polished using linisher polisher followed by different grades of emery sheets (1/0 and 2/0) to obtain a good surface finish and then with a disc polisher in the presence of diluted $Al_2O_3$ to attain the fine surface finish which would allow clear observation of the reinforcement particles in the matrix. Each specimen was etched using Keller's reagent prior to examination in a Zeiss Axiovert 25 CA Inverted Metallurgical Microscope (Carl Zeiss AG, Oberkochen, Germany).

### 2.4 Response Surface Methodology

RSM is a mathematical and statistical method used for modeling and identifying clear relationships between the parameters and response with a minimum number of experiments [11]. This method is used here to study the relationship between the parameters (load, velocity and sliding distance) and the response (dry sliding wear characteristics). A second order polynomial regression model is constructed to predict the relationship, which is shown in Eq. (1).

$$Y_u = b + \sum b_I x_{iu} + \sum b_{ii} x_{iu}^2 + \sum b_{ij} x_{iu} x_{ju} \qquad (1)$$

where $Y_u$ is the response and $b$, $b_I$, $b_{ii}$, and $b_{ij}$ are the coefficients. The second term denotes the linear effect, the third term denotes the higher order effect and the fourth term denotes the interaction effect.

The selection of experiments and the analyses were carried out using the statistical software Minitab version 15 (Minitab Inc., State College, PA). A central composite design (CCD) was selected for determining the dry sliding wear characteristics of the fabricated composite. In the RSM, the number of parameters determines the number of experimental runs. For the three parameters (load, velocity and sliding distance) selected in this study, 20 experimental runs were generated. A high and low level of load (10 and 50 N), velocity (1 and 5 m/s) and sliding distance (500 and 1500 m) were used as input in the CCD, and an experimental design was obtained with each parameter varied at five levels. The layout of the process parameters and their levels are shown in Table 2.

## 2.5 Dry Sliding Wear Test

Specimens measuring $8 \times 8 \times 35$ mm were taken from the Al–Si12Cu/TiB$_2$ composite for the dry sliding wear test. This test was performed using a pin-on-disc tribometer (Fig. 1) in the unlubricated condition of the specimen/disc interface. This tribometer consisted of a hardened counterface made of EN31 steel (C, 1.08 %; Si, 0.25 %; Mn, 0.53 %; S, 0.015 %; P, 0.022 %; Ni, 0.33 %; Cr, 1.46 %; Mo, 0.06 %; hardness of 60 HRC). The disc rotates and thereby produces sliding wear as the specimen adheres to it; load is applied through the lever and results in continuous contact between the specimen and the counterface. The specimens were first cleaned and the counterface also polished using emery sheets to obtain fresh surface contact between the two. The experiments were conducted as per the design determined using RSM. The specimens were weighed before and after the experiment using a precision weighing balance to predict the mass loss, and the volumetric wear rate was calculated based on the mass loss using the formula

$$W = \frac{M}{\rho D} \tag{2}$$

where $W$ is the wear rate (mm$^3$/m), $M$ is mass loss (g), $\rho$ is density (g/mm$^3$) and $D$ is the sliding distance (m).

As the reinforcement weight percentage (wt%) was kept constant (10 wt%) during the fabrication process, the

Table 2 Experimental layout of process parameters and their levels

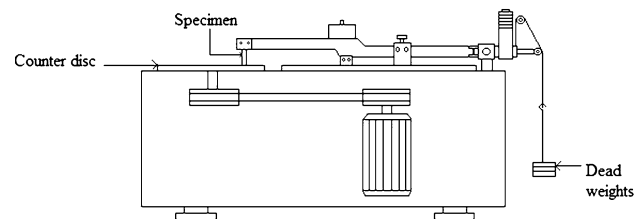| Factors | Levels | | | | |
|---|---|---|---|---|---|
| Load (N) | 10 | 18 | 30 | 42 | 50 |
| Velocity (m/s) | 1.0 | 1.8 | 3.0 | 4.1 | 5.0 |
| Sliding distance (m) | 500 | 905 | 1500 | 2095 | 2500 |



Fig. 1 Schematic illustration of pin on disc tribometer

densities of the composite specimens did not vary to any significant extent. In addition, as the wear process parameters were varied for each experiment, the volumetric wear rates were calculated.

According to Archard's law, the wear rate is directly proportional to load and the sliding distance, as given in Eq. (3)

$$W = K \times L \times D \tag{3}$$

where $W$ is the sliding wear, $K$ is the wear coefficient, $L$ is the normal load and $D$ is the sliding distance (m). As this law may not be suitable for the wear behaviour of all the materials, the wear experiments were conducted using a statistical approach to determine the effect of load and sliding distance on variations in the wear rate of the Al/TiB$_2$ composite.

## 3 Results and Discussion

The following sections briefly describe the microstructural investigation, dry sliding wear behaviour and scanning electron microscopy (SEM) analysis.

### 3.1 Microstructural Investigation

The optical micrograph of the Al–Si12Cu/TiB$_2$ MMC is shown in Fig. 2, where it can be seen that the particles are dispersed evenly throughout the matrix due to the adequate stirring speed of 200 rpm. Sufficient agitation helps to break down the oxide layers formed in the molten metal and allows for wettability of the molten metal with the reinforcement particles. Consequently, the aluminium molten metal spreads around the particles and forms good wettability. This result shows that uniform dispersion can be achieved by including a stirring step in this liquid metallurgy technique; the same result was obtained by Singla et al. [12].

### 3.2 Dry Sliding Wear Characteristics

The wear rate of the AMMC according to the results of the dry sliding experiments in which three parameters (load, velocity and sliding distance) were varied are shown in
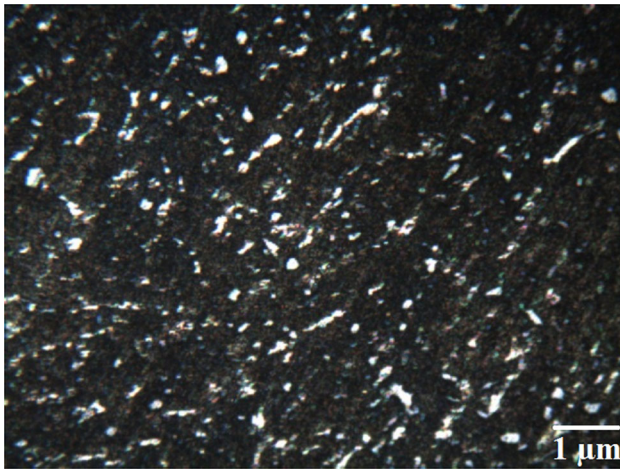
**Fig. 2** Microstructure of the Al–Si12Cu/TiB$_2$ composite

Table 3. Each test was repeated five times and the average value of the wear rate is shown. The incorporation of hard TiB$_2$ particles in the high wear-resistant Al–Si12Cu alloy resulted in a minimum mass loss of material during the wear test. This small difference is accounted by measuring the mass using a precision electronic weighing balance at an accuracy of 0.1 mg. Hence, the wear rates are calculated at high precision.

In this study, the pin was constructed from aluminium composite and the disc was made of steel. The wear results would not be the same if the pin were to be made of steel and the disc of aluminium composite because even slight

variations in a tribo system cause greater variations in the wear rates as the latter depend on various parametrical conditions [13]. Higher wear rates would appear with the aluminium composite even if the inverse configuration were to be used because the softer material experiences more wear when two dissimilar materials of different hardness slide against each other [14].

The wear behaviour was analyzed using Minitab version 15, and the regression coefficients obtained using the significance test are shown in Table 4. The $R^2$ and adjusted $R^2$ obtained from the significance test were 92.9 and 86.6 %, respectively, which are quite close to each other. This minor difference in value shows that the developed model predicts well the relation between the dry sliding wear characteristics and the process parameters, such as load, velocity and sliding distance.

Those terms with a $p$ value of $<0.05$ had a highly significant effect on the wear rate. The higher level of velocity ($P = 0.002$) was found to have the most significant effect on the wear rate, with load and velocity having a less significant effect. Those terms with a $p$ value of $>0.10$ were not significant. Therefore, the obtained model for wear rate was

$$0.001836 + 0.000058\,L - 0.000660\,V + 0.000161\,V \times V - 0.000004\,L \times V$$

$$(4)$$

The model shows the extent of significance of the linear terms, square terms and interaction terms on the wear rate.

**Table 3** Experimental design and the results of varying load, velocity and sliding distance on wear rate

| Specimen no. | Load (N) | Velocity (m/s) | Sliding distance (m) | Wear rate (mm$^3$/m) |
|---|---|---|---|---|
| 1 | 30 | 3.0 | 1500 | 0.0029 |
| 2 | 18 | 1.8 | 2095 | 0.0024 |
| 3 | 42 | 4.1 | 2095 | 0.0035 |
| 4 | 30 | 5.0 | 1500 | 0.0039 |
| 5 | 18 | 4.1 | 2095 | 0.0029 |
| 6 | 30 | 3.0 | 1500 | 0.0029 |
| 7 | 30 | 3.0 | 1500 | 0.0026 |
| 8 | 18 | 4.1 | 905 | 0.0030 |
| 9 | 30 | 3.0 | 1500 | 0.0027 |
| 10 | 30 | 3.0 | 500 | 0.0029 |
| 11 | 10 | 3.0 | 1500 | 0.0018 |
| 12 | 30 | 3.0 | 1500 | 0.0030 |
| 13 | 42 | 4.1 | 905 | 0.0038 |
| 14 | 30 | 3.0 | 2500 | 0.0025 |
| 15 | 18 | 1.8 | 905 | 0.0023 |
| 16 | 50 | 3.0 | 1500 | 0.0040 |
| 17 | 42 | 1.8 | 2095 | 0.0030 |
| 18 | 42 | 1.8 | 905 | 0.0035 |
| 19 | 30 | 1.0 | 1500 | 0.0030 |
| 20 | 30 | 3.0 | 1500 | 0.0027 |

**Table 4** Estimated regression coefficients for wear rate

| Term | Coefficient | Standard error coefficient | T | p |
|---|---|---|---|---|
| Constant | 0.001836 | 0.001005 | 1.826 | 0.098 |
| Load (N) | 0.000058 | 0.000032 | 1.855 | 0.093 |
| Velocity (m/s) | −0.000660 | 0.000315 | −2.094 | 0.063 |
| Sliding distance (m) | 0.000000 | 0.000001 | 0.538 | 0.602 |
| Load (N) × load (N) | 0.000000 | 0.000000 | 0.687 | 0.507 |
| Velocity (m/s) × velocity (m/s) | 0.000161 | 0.000038 | 4.269 | 0.002* |
| Sliding distance (m) × sliding distance (m) | −0.000000 | 0.000000 | −0.341 | 0.740 |
| Load (N) × velocity (m/s) | −0.000004 | 0.000005 | −0.769 | 0.460 |
| Load (N) × sliding distance (m) | 0.000000 | 0.000000 | −1.293 | 0.225 |
| Velocity (m/s) × sliding distance (m) | 0.000000 | 0.000000 | 0.140 | 0.892 |

* Significant at $p < 0.05$

$T$ $t$ test

From the model, it can be determined that the linear terms and square terms had a more significant effect on the wear rate than the interaction terms of the parameters. Among the interaction terms, the mutual effect of $L \times V$ had a significant effect on the wear rate, as seen from Eq. (4). The regression model developed using the obtained regression coefficients were checked for adequacy in the confirmation experiments where a new set of parameters were used in the model and the model results then compared with the experimental results obtained for the new levels. The new level of parameters selected for the adequacy checking, regression model wear rate and experimental wear rate are shown in Table 5. The values of the levels selected differed from the parametric values used in the experimental conditions generated through CCD.

The error percentage was predicted based on the comparison of wear rate determined using the experimental results and those from the regression model. The error percentage of <7 % confirms that the developed model predicted the dry sliding wear characteristics of the developed composite with high accuracy. The model was developed only for the range of parameters defined in this study, as well as only for the range of wear rate values obtained in this study. Within this framework, this model was highly efficient and will retain its good accuracy when a large range of parameters are selected.

The significance of each term in the regression model was checked using analysis of variance (ANOVA) at the 5 % significance level and 95 % confidence level (Table 6). The significance of a model, the coefficient terms and lack of fit can be predicted using ANOVA to determine the accuracy of the developed model [15]. The lack of fit has an $F$ value of 2.76, which is less than the standard $F$ value of 5.05 for the 95 % confidence level, thereby demonstrating that the developed model is adequate.

The surface plots for wear rate were generated for all pairs of process parameters (Figs. 3–5). The surface plot shows that wear rate increased with increasing load at all levels of velocity (Fig. 3) and at all levels of sliding distance (Fig. 5), in correspondence to the variations in the linear closeness between the two metallic surfaces due to variations in the load. A load applied externally onto a specimen deforms the surface of that specimen when it comes into continuous contact with the counterface. The load generally increases the contact of the specimen with the counterface, which in turn increases the temperature at the interface, thereby resulting in increased wear rate; the same behaviour observed in our study has been seen in other studies [16, 17]. The surface plot (Fig. 3) shows that the wear rate decreased initially and then increased, reaching a peak at high velocity with respect to load. This can be attributed to the increased contact time of the specimen with the counterface at low velocity which results in high metallic contact and a high observed wear rate. When the velocity increases, the temperature at the interface would increase and an oxide layer, called a mechanical

**Table 5** Comparison of wear rate determined using experimental results and regression analysis

| Specimen no. | Load (N) | Velocity (m/s) | Sliding distance (m) | Experimental wear rate (mm³/m) | Regression wear rate (mm³/m) | Error (%) |
|---|---|---|---|---|---|---|
| 1 | 15 | 1.5 | 800 | 0.00198 | 0.00185 | 6.56 |
| 2 | 25 | 2.5 | 1600 | 0.00239 | 0.00226 | 5.43 |
| 3 | 45 | 4.5 | 2400 | 0.00392 | 0.00383 | 2.29 |

**Table 6** Analysis of variance for wear rate

| Source | df | Seq. SS | Adj. SS | Adj. MS | F | p |
|---|---|---|---|---|---|---|
| Regression | 9 | 0.000005 | 0.000005 | 0.000001 | 14.59 | 0.000 |
| Linear | 3 | 0.000005 | 0.000000 | 0.000000 | 3.77 | 0.048 |
| Square | 3 | 0.000001 | 0.000001 | 0.000000 | 6.31 | 0.011 |
| Interaction | 3 | 0.000000 | 0.000000 | 0.000000 | 0.76 | 0.541 |
| Residual error | 10 | 0.000000 | 0.000000 | 0.000000 | | |
| Lack of fit | 5 | 0.000000 | 0.000000 | 0.000000 | 2.76 | 0.145 |
| Pure error | 5 | 0.000000 | 0.000000 | 0.000000 | | |
| Total | 19 | 0.000006 | | | | |

*Seq. SS* Sequential sum of squares, *Adj. SS* adjacent sum of squares, *Adj. MS* adjacent mean squares, *F* Fisher's test, *P* Percentage
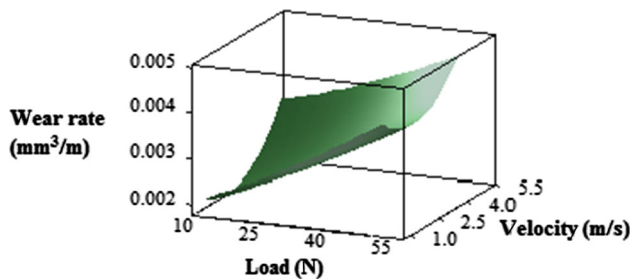


**Fig. 3** Surface plot of wear rate as a function of load and velocity for a constant sliding distance of 1500 m
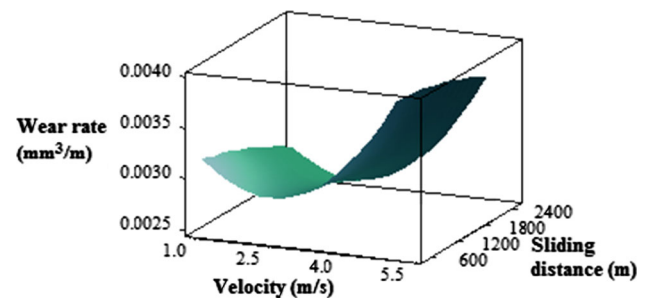


**Fig. 4** Surface plot of wear rate as a function of velocity and sliding distance for a constant load of 30 N

mixed layer (MML), might form over the surface of the specimen due to the transfer of materials; the same mechanism has been observed in other studies [18, 19].This layer protects the specimen from the adhesion wear caused during sliding and, thereby, the wear rate was found to decrease initially. Following this condition, a transition took place in the wear rate which might be due to the breakdown of the unstable MML with increasing load on the specimen; a high wear rate is observed at the velocity of 5 m/s and the high load of 50 N; the same trend has been seen in a previous study [20]. This trend is attributed to the combined effect of high load and high velocity which produces a great pressure on the steel disc along with material loss from the specimen. The surface plots (Figs. 3, 4) can be seen to have a curvature effect which reveals that non-linear variation of wear rate occurred due to the combination of different parameters. The curvature behaviour depends on the significance of the particular combination of the parameters [21].

The same trend of wear rate (Fig. 4) was observed for changes in velocity with respect to the sliding distance. The surface plots shows that wear rate slightly decreased with increasing sliding distance with respect to velocity (Fig. 4) and load (Fig. 5), respectively. Hard reinforcement particles which protrude at the matrix surface will tend to come into contact with the counterface at the initial sliding

distance. In our study, these protrusions produce uneven contact and result in even more material removal. With increasing sliding distance, the sharp hard asperities at the specimen surface had smoothed out after being run for a certain sliding distance. When this same mechanism was observed in other studies, uniform contact occurred at the interface, producing a lower wear rate of the specimen [22, 23].

## 3.3 Optimization of Response

Optimization of the responses using the RSM technique identified the process parameters which would result in a
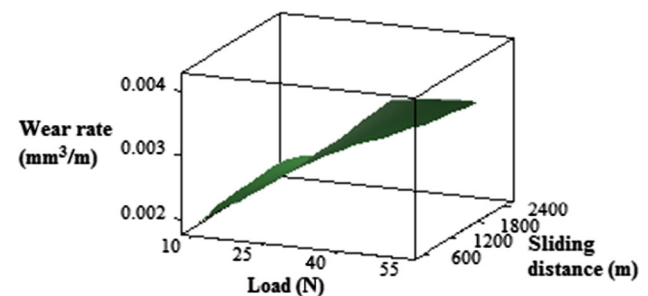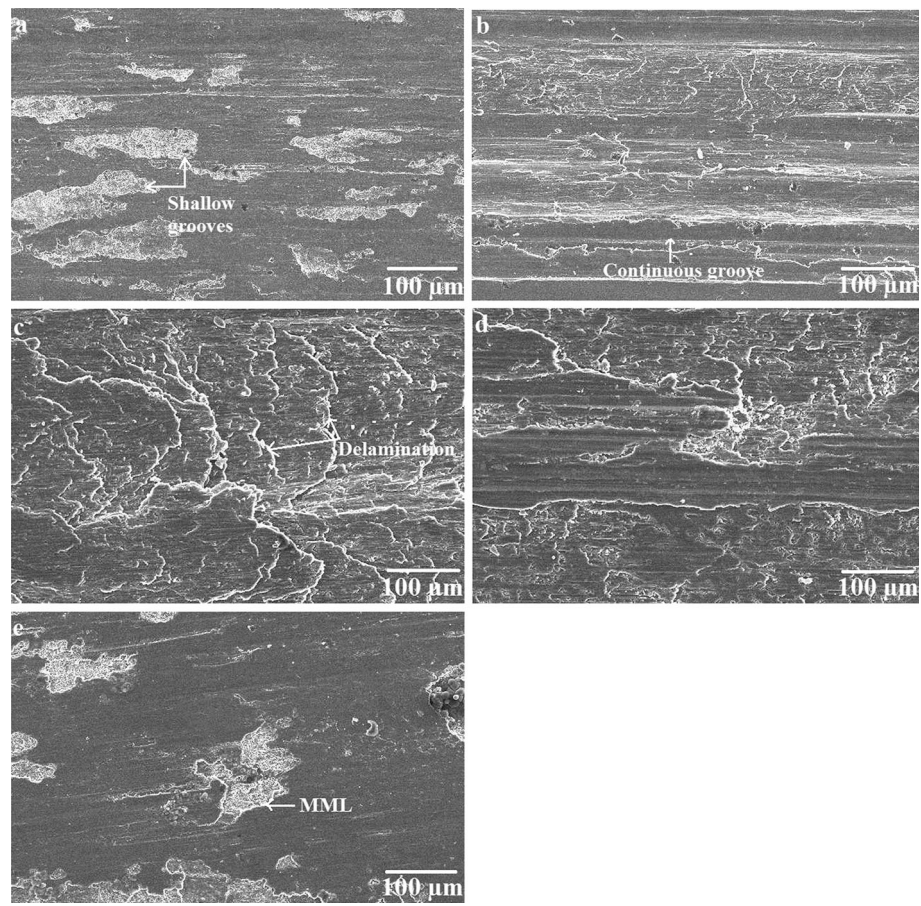


**Fig. 5** Surface plot of wear rate as a function of load and sliding distance for a constant velocity of 3 m/s

**Fig. 6** Worn surfaces of Al–Si12Cu/TiB$_2$ composite specimens under various conditions: **a** $L = 10$ N, $V = 3$ m/s, $D = 1500$ m; **b** $L = 30$ N, $V = 3$ m/s, $D = 1500$ m; **c** $L = 50$ N, $V = 3$ m/s, $D = 1500$ m; **d** $L = 30$ N, $V = 1$ m/s, $D = 1500$ m; **e** $L = 30$ N, $V = 3$ m/s, $D = 500$ m. $L$ Load, $V$ velocity $D$ sliding distance



lower wear rate by determining the relationship between the parameters, such as load, velocity and sliding distance, and the dry sliding wear behaviour of the developed AMMC. The aim of this optimization process was to minimize the dry sliding wear. The target and the upper bound were used as inputs in the optimization process, and the global solution for obtaining the targeted wear rate of 0.00179 mm$^3$/m were a load of 10 N, velocity of 2.226 m/s and sliding distance of 500 m.

### 3.4 SEM Analysis

The worn surfaces of the Al–Si12Cu/TiB$_2$ composite specimens are shown in Fig. 6a–e. The worn surfaces reveal the wear mechanisms that resulted from the dry sliding wear test. Figure 6a–c shows the wear mechanisms during the transition of load onto the surface of the composite specimens at a constant velocity and constant sliding distance of 3 m/s and 1500 m, respectively. The surface of the composite specimen (Fig. 6a) can be seen to be worn down at a low load (10 N), with scratches and shallow grooves at a few areas, resulting in a lower wear rate due to the avoidance of contact between the aluminium matrix and the counterface by the action of the reinforcement particles

as the load-bearing elements. These load-bearing elements would bear the total load prevent the transfer of the load to the matrix, resulting in a lower wear rate. The worn surface (Fig. 6b) at the load of 30 N can be seen to have continuous grooves in the sliding direction of the specimen over the surface. Material would have removed when the real contact increased with increasing load, and this removed material would have rolled between the two surfaces, ultimately ending up somewhere on the surface of the specimen. The continuous rotating of the counterface would cause this material to slide along the specimen surface, producing continuous grooves on the specimen surface until it detached from the specimen surface, thereby resulting in more material removal. The worn surface (Fig. 6c) at the high load (50 N) can be seen to suffer from severe delamination, probably caused by the formation of high temperature at the interfaces. A high temperature at a high load of 50 N may be due to the frictional heat generation between two surfaces under heavy contact, which would cause a high level of deformation of the material and result in more material removal. Thus, mild adhesion was followed by severe delamination with increasing load. This result confirms the wear trend observed in the surface plots (Figs. 3, 5) and shows that the

wear rate increased linearly with increasing load; the same mechanism was observed in a previous study [24].

In general, an increase in wear rate was observed with increasing load, but the severity of wear was delayed at all load conditions, most likely due to the surface hardness of the composite. This composite had a surface hardness of 118 HV, and therefore it was able to resist the amount of deformation produced at all loads. The hardness imparted by the $TiB_2$ reinforcement particles reduced the severity of the wear on the surface, resulting in less wear at all conditions. This lower wear can be related to several material parameters and processing parameters. The AlSi12Cu alloy has a high silicon content of 10.9 %, and it is commonly known that a higher silicon content imparts a higher wear resistance to the alloy. The preheating of the $TiB_2$ reinforcement particles, stirring of these particles in the molten metal at 200 rpm for 5 min and the size of the $TiB_2$ particles (neither fine nor coarse) resulted in the absence of agglomeration and uniform dispersion of the reinforcement particles throughout the matrix. Also, the wettability promoted by the silicon and magnesium content in this aluminium alloy resulted in good bonding of the reinforcement particles in the matrix. This uniform dispersion and good bonding of $TiB_2$ reinforcement particles in the composite resulted in a lower order of wear rate at all test conditions.

The transition of the wear mechanism of the composite specimen from a velocity of 1 to 3 m/s demonstrates the role of MML in the wear process (Fig. 6d, e). The worn surface shown in Fig. 6d (velocity 1 m/s) is characterized by the removal of more material than that shown in Fig. 6e (3 m/s), and this larger amount of removed material is attributable to the low velocity causing a long contact time between the specimen and the counterface. In our study, this condition facilitated sufficient contact between the total area of the specimen surface and the counterface and
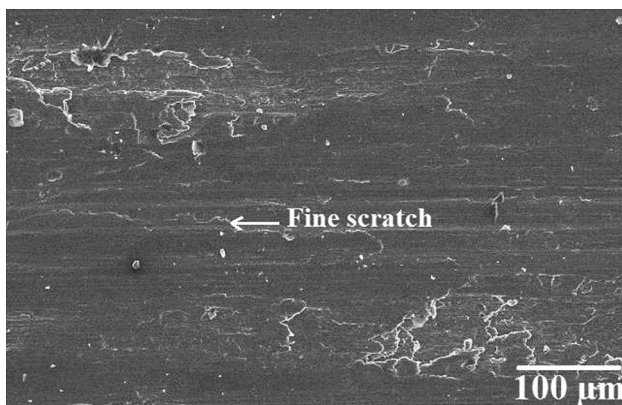
resulted in a higher wear rate. The worn surface subjected to the velocity of 3 m/s (Fig. 6e) shows the formation of the MML, due to the increased velocity of the counterface. This higher velocity induced a high temperature at the interfaces which in turn softened the specimen. The softened material reacted with the oxygen and formed a thick oxide layer at the specimen surface which acts as a solid lubricant and protects the surface from severe wear, resulting in a lower wear rate; the same phenomena have been seen in a previous study [25].

The accuracy of the developed model was checked by studying the surface worn at the optimum condition by SEM analysis. The surface worn at load of 1 N, velocity of 2.2 m/s and sliding distance of 500 m is shown in Fig. 7. Very small scratches can be observed on the surface of the specimen at a few place, resulting in a minimum wear rate, which ensures the accuracy of the developed model.

# 4 Conclusion

The Al–Si12Cu/$TiB_2$ metal matrix composite was fabricated successfully by achieving a uniform dispersion of reinforcement particles in the matrix, which was verified in the optical micrograph. The developed model was found to perform well in terms of predicting the dry sliding wear behaviour of the Al–Si12Cu/$TiB_2$ composite with good accuracy. The regression test showed that a higher order of velocity significantly affected the wear rate of the composite. The confirmatory test revealed that the developed model is accurate with a relatively lower percentage of error. The surface plots shows that wear rate increased with increasing load, decreased with increasing sliding distance and nonlinearly varied with respect to velocity. The optimized parameters, which were identified in the optimization study to result in a minimum wear rate, were a load of 10 N, velocity of 2.226 m/s and sliding distance of 500 m. A study of the worn surfaces revealed that load played an important role in controlling the wear mechanisms and also revealed that the mechanically mixed layer protected the composite specimen from material removal. This developed MMC with good wear resistance can be used for the improvement of wear performance in automotive engine pistons.



**Fig. 7** Surface worn at optimum condition $L = 10$ N, $V = 2.2$ m/s, $D = 500$ m

# References

1. Sudarshan, Surappa, M.K.: Dry sliding wear of fly ash particle reinforced A356 Al composites. Wear **265**, 349–360 (2008)
2. Uthayakumar, M., Aravindan, S., Rajkumar, K.: Wear performance of Al–SiC–$B_4$C hybrid composites under dry sliding conditions. Mater. Des. **47**, 456–464 (2013)

3. Meena, K.L., Manna, A., Banwait, S.S., Jaswanti, : An analysis of mechanical properties of the developed Al/SiC-MMC's. Am. J. Mech. Eng. **1**, 14–19 (2013)

4. Sucitharan, K.S., SenthilKumar, P., Shivalingappa, D., Jenix Rino, J.: Wear behaviour of Al6063-zircon sand metal matrix composite. IOSR J. Eng. **3**, 24–28 (2013)

5. Magesh, M., John Baruch, L., George Oliver, D.: Microstructure and hardness of aluminium alloy-fused silica particulate composite. Int. J. Innov. Res. Adv. Eng. **1**, 199–204 (2014)

6. Sasikumar, S., Ramkumar, K.R., Iniyan, S., Gowthaman, M., Sivasankaran, S.: Study of mechanical and machining behavior of AA7075-3%TiB$_2$ in situ composite. Int. J. Innov. Res. Sci. Eng. Technol. **3**, 1229–1233 (2014)

7. Bhaskar, H.B., Sharief, A.: Dry sliding wear behaviour of aluminium/Be$_3$Al$_2$(SiO$_3$)$_6$ composite using Taguchi method. J. Miner. Mater. Charact. Eng. **11**, 679–684 (2012)

8. Kundu, S., Roy, B.K., Mishra, A.K.: Study of dry sliding wear behavior of aluminium/SiC/Al$_2$O$_3$/graphite hybrid metal matrix composite using Taguchi technique. Int. J. Sci. Res. Publ. **3**, 1–8 (2013)

9. Mishra, Punyapriya: Statistical analysis for the abrasive wear behavior of bagasse fiber reinforced polymer composite. Int. J. Appl. Res. Mech. Eng. **2**, 7–11 (2012)

10. Bayhan, M., Onel, K.: Optimization of reinforcement content and sliding distance for AlSi7Mg/SiC$_p$ composites using response surface methodology. Mater. Des. **31**, 3015–3022 (2010)

11. Vettivel, S.C., Selvakumar, N., Narayanasamy, R., Leema, N.: Numerical modelling, prediction of Cu–W nano powder composite in dry sliding wear condition using response surface methodology. Mater. Des. **50**, 977–996 (2013)

12. Singla, M., Dwivedi, D.D., Singh, L., Chawla, V.: Development of aluminium based silicon carbide particulate metal matrix composite. J. Miner. Mater. Charact. Eng. **8**, 455–467 (2009)

13. Kato, K., Adachi, K.: Wear Mechanisms. CRC Press LLC, Boca Raton (2001)

14. So, H.: Characteristics of wear results tested by pin-on-disc at moderate to high speeds. Tribol. Int. **29**(5), 415–423 (1996)

15. Sharma, Satpal: Parametric study of abrasive wear of Co–CrC based flame sprayed coatings by Response Surface Methodology. Tribol. Int. **75**, 39–50 (2014)

16. Dwivedi, D.K.: Adhesive wear behaviour of cast aluminium–silicon alloys: overview. Mater. Des. **31**, 2517–2531 (2010)

17. Baradeswaran, A., Elaya Perumal, A.: Influence of B$_4$C on the tribological and mechanical properties of Al 7075–B$_4$C composites. Compos. Part B **54**, 146–152 (2013)

18. Jo, S.K., Lee, W.J., Park, Y.H., Park, I.M.: Effect of SiC particle size on wear properties of Al$_2$O$_3$·SiO$_2$/SiC/Mg hybrid metal matrix composites. Tribol. Lett. **45**, 101–107 (2012)

19. Radhika, N., Subramanian, R.: Effect of reinforcement on wear behaviour of aluminium hybrid composites. Tribol. Mater. Surf. Interfaces **7**(1), 36–41 (2013)

20. Basavarajappa, Satyappa, Chandramohan, G.: Dry sliding wear behaviour of hybrid metal matrix composites. Mater. Sci. **11**, 253–257 (2005)

21. Janardhan, M.: Multi-response optimization of EDM performance characteristics using response surface methodology and desirability function. ARPN J. Eng. Appl. Sci. **9**, 12 (2014)

22. Zhang, L., He, X.B., Qu, X.H., Duan, B.H., Lu, X., Qin, M.L.: Dry sliding wear properties of high volume fraction SiC$_p$/Cu composites produced by pressure less infiltration. Wear **265**, 1848–1856 (2008)

23. Kaur, K., Anant, R., Pandey, O.P.: Tribological behaviour of SiC particle reinforced Al–Si alloy. Tribol. Lett. **44**, 41–58 (2011)

24. Cui, Gongjun, Niu, Muye, Zhu, Shengyu, Yang, Jun, Bi, Qinling: Dry-sliding tribological properties of bronze–graphite composites. Tribol. Lett. **48**, 111–122 (2012)

25. Veeresh Kumar, G.B., Rao, C.S.P., Selvaraj, N.: Mechanical and tribological behavior of particulate reinforced aluminium metal matrix composites—a review. J. Miner. Mater. Charact. Eng. **10**, 59–91 (2011)